Solar Energy 222 (2021) 84–94

Contents lists available at ScienceDirect

Solar Energy

journal homepage: www.elsevier.com/locate/solener

Degradation analysis of photovoltaic modules after operating for 22 years. A case study with comparisons

L. Lillo-Sánchez [a,*], G. López-Lara [b], J. Vera-Medina [c], E. Pérez-Aparicio [d], I. Lillo-Bravo [a]

[a] Department of Energy Engineering, University of Seville, Seville, Spain
[b] Technological Corporation of Andalusia (CTA), Seville, Spain
[c] Solar Thermal Energy Department, National Renewable Energy Centre (CENER), Seville, Spain
[d] Andalusian Association for Research and Industrial Cooperation (AICIA), Seville, Spain

ARTICLE INFO

Keywords:
Photovoltaic module performance
Long-term degradation
Electroluminiscence
Photovoltaic module warranty

ABSTRACT

The analysis of degradation mechanisms of photovoltaic (PV) modules is key to ensure its current lifetime and the economic feasibility of PV systems. Field operation is the best way to observe and detect all type of degradation mechanisms. This paper presents the main signs of degradation on 56 m-Si PV modules caused by outdoor exposure after a period of 22 years in Seville, Spain. Results are compared with other research works conclusions that analyse the degradation of identical PV cells and same manufacturer, after an exposure period of 12, 15 and 17 years. The analysis was conducted by visual inspection, infrared thermography, electroluminescence (EL) and electrical performance evaluation. The mean peak power degradation has been 30,9% in the 22 operation years, equivalent to 1,4% per year, which corresponds mainly to a loss in short-circuit current and, in a less degree, to loss in fill factor and open circuit voltage. The most significant defects found were severe browning, milky pattern and oxidation of the metallization grid. Those defects seem turns severe failures when exposure period is more than about 20 years and could explain the high degradation rate based on a comparison performed with other research works.

1. Introduction

The PV systems market is rapidly expanding to significant penetrations in grid-connected markets in an increasing number of countries (International Energy Agency, 2019). To support this market expansion, it is required the access to reliable information on the performance and sustainability of PV systems because they have a direct impact on the estimation of the financial return on investment, the levelized cost of energy (Jordan et al., 2016) and the possible warranty claims according to photovoltaic module manufacturerś specifications (LG, 2020; SUNPOWER, 2020).

A thorough understanding of PV module degradation mechanisms and field operation rates are required to promote this market expansion.

Degradation of PV modules leads to results in generation of various types of defects in the frame, junction box, front and back side of the PV module. The most frequent defects are encapsulant browning, hot spots, milky pattern, delamination and bubble formation in the encapsulant, back sheet polymer cracks, junction box connections corrosion, busbar, front grid and anti-reflection coating corrosion and discoloration and junction cables insulation degradation (Jahn et al., 2018) affecting, with other failures of the PV system, to the energy yield (Lillo-Bravo et al., 2018).

According to IEA-PVPS TASK13-01 (2014) and (Jahn et al., 2018), in the initial period of operation, degradation rates of the nominal power tend to be higher than during the rest of the operating life due to the stronger action of specific degradation modes, such as light induced degradation (LID), glass breakage, contact failures in the junction box and string interconnects and loose frame. Other defects, at a lower level, are potencial induced degradation, diode failure and cell interconnect breakage. The ethilen-vinil acetate (EVA) discoloration, delamination, antireflecting (AR) layer degradation and cracked cell in turn, mainly affects the degradation rate of the nominal power during its mid-life period, reducing the short circuit current of the modules. Oxidation affects significantly the module during last years of life.

Degradation of PV modules is highly dependent on the climate (Mussard and Amara, 2018) but also depends on lamination materials,

* Corresponding author at: Department of Energy Engineering, Escuela Técnica Superior de Ingeniería, University of Seville, Camino de los Descubrimientos s/n. 41092, Seville, Spain.
E-mail address: laura-lillo@alum.us.es (L. Lillo-Sánchez).

https://doi.org/10.1016/j.solener.2021.04.026
Received 18 February 2021; Received in revised form 6 April 2021; Accepted 9 April 2021
Available online 17 May 2021

solar module processing, aggressive environmental parameters, PV technology, period of exposition, the installation method, solar tracking system, solar radiation concentration mechanism and PV system voltage. Dubey et al. (2013) observed that discoloured PV modules tend to correlate with hot and dry climates, while corrosion is more common in hot and humid zones. It also depends on lamination materials, cell technology and manufacturing technology (Sharma et al., 2014). IEA-PVPS T13-09: 2017 (Köntges et al., 2017) shows that in most cases interactions between materials in the PV module are the main root cause for PV module degradation. Ndiaye et al. (2013) points out that corrosion and discoloration are the predominant modes of PV module degradation. To a lesser extent, degradation of PV modules depends on the installation method -specially in BIPV applications- solar tracking system, solar radiation concentration mechanism and PV systems voltage (Jordan et al., 2017a).

The qualification tests for PV modules are performed mostly according to the standards IEC 61215-1(2016), IEC 61215-2 (2016); IEC 61215 1-1(2016) until EC 61215 1-4 (2016). Those tests do not have the ability to reproduce all degradation modes observed in real-time field exposure (Jorgensen et al., 2003) nor to predict the degradation of a specific PV module failure what remains a challenging task (Köntges et al., 2017). As modeling of PV performance becomes more sophisticated, degradation rates based on the assumption of linearity may not be enough accurate. Non-linear trends at the beginning of lifespan or during the wear-out phase are important to detect and understand PV systems economically and technically (Jordan et al., 2017b). Although different statistical and analytical methods for the prediction of PV modules degradation rates (Gu et al., 2015; Braisaz et al., 2014; Pan et al., 2011; Zimmermann, 2008) have been proposed, a more accurate prediction of PV module performance and the capability of linking performance losses to relevant degradation modes is required (Ndiaye et al., 2013; Lindig et al., 2018). Therefore, it is required and necessary additional data and deeper analyses of the reliability and performance degradation of PV modules after a long-term field exposure under different scenarios using better tools (Jahn et al., 2018). Berardone et al. (2018) point that there are still few studies employing EL and infrared (IR) imagery.

Studies on PV modules degradation carried out over the last 40 years show that the mean power degradation rate depends on the number of years of operation, encapsulant, climate and assembly type. In the case of crystalline silicon cells range between 0.5 and 1.9%/year have been observed (Sharma et al., 2014).

Pramod et al. (2016) reported that after 22 years outdoor exposure of 90 m-C-Si technology PV modules with nominal power 40 Wp in a composite climate of India that the degradation rate of the peak power has been an average value 1,9%/year. The defects in busbar, cell interconnection ribbon, string inter-connection ribbon and chalking in backsheet were the most frequently observed defects. Chandel et al. (2015) reported that after 28 years outdoor exposure of 12 mono-C- Si technology PV modules with nominal power 33 Wp for western Himalayan region of Indian climate that have 1,4%/year average power degradation. Main defects observed in PV modules are encapsulant discolouration, delamination, oxidation of front grid fingers and anti-reflective coating, glass breakage and bubbles in back sheet.

Due to their direct relation with this work, the studies carried out by Sánchez-Friera et al. (2011), Moreton et al. (2013) and Ferreira da Fonseca et al. (2020) are specially interesting. Those three works analyse the PV modules degradation from the same manufacturer Isofoton, with the same mC-Si cell, 103x103 mm size, manufacturing process and encapsulant that this study. These studies, located in three different sites, Malaga (Spain), Porto Alegre (Brasil) and Madrid (Spain) and with different number of operation years, 12, 15 and 17 respectively show slightly different results.

The specific objectives of this work are to evaluate the defects and degradation rates of 56 PV modules manufactured by Isofoton, made up of m-C Si cells, 103x103 mm size and that have operated for 22 years in the city of Seville, located at the South of Spain and to compare the obtained results with the ones of reference studies mentioned above.

The paper is structured as follows: In Section 2 we describe the PV modules and inspections methods. Section 3 shows the results and discussion. Section 4 shows the comparative analysis with other research works. The main conclusions of this study are outlined in Section 5.

2. PV modules and inspection methods.

It has been analysed a set of 56 PV modules manufactured by Isofoton (Spain) in 1991, model M−55−L with the nominal characteristics in standard test conditions (STC), (incident power density: 1000 W/m^2, spectrum: AM 1,5G, module temperature: 25 °C) of P_{mp} = 53 Wp, I_{SC} = 3,27 A and V_{OC} = 21,8 V, Imp = 3,05 A and V_{mp} = 17,4 V, fill factor (FF), FF = 0,743 and efficiency of 12,74% . The Nominal Operating Cell Temperature (NOCT) of the PV module is 47 °C and dimensions of 1330 mm × 340 mm. This module is composed of 36 series-connected monocrystalline silicon solar cells of size 103 mm and about 300 μm thickness. The cells are textured and have a TiOx antireflecting coating. They are interconnected with tinned copper ribbons. The cells are encapsulated with EVA between a high transmittance flat tempered glass and a composite backsheet of a polyvinyl fluoride (PVF) film, also called Tedlar, and polyester (PET), with a PVF/PET/PVF configuration. It was extensively used as back-sheet for PV modules until about 2010 when cheaper multi-layer films having similar properties and resistance to weather were developed. Each module contains two IP 65 protected junction boxes with by-pass diodes in parallel with 24 cells. The laminate is surrounded by an anodized aluminium frame, with a silicone joint.

Those modules were installed in two different locations in Seville (Spain). From August 1991 to July 2001 they were installed in a location whose coordinates are 37°24′26.9″N 6°00′08.8″W. Those modules were part of a network connection installation for the lighting of the Spanish Pavilion offices of the Universal Exposition of Seville (1992). From July 2001 to July 2007 the modules were stored without being connected in an enclosed place. From November 2007 to March 2020 they were operating on the roof of a house sited in Seville, whose coordinates are 37°20′54.7″N 5°59′05.9″W. The distance between both locations is 8 km in a straight line. Fig. 1 shows a general view of the installation and a close view of the PV modules.

The PV field of the Spanish Pavilion had a total peak power of 27,67 kWp, made up of 522 PV modules, arranged in 18 parallel rows of 29 serie-connected PV modules each, on a horizontal surface on the roof of the Pavilion offices. It also had 29 gel batteries of C_{10} = 155 Ah, 12 V, a voltage regulator and a 25 kW single-phase inverter whose input voltage range is 300 /405 V and output voltage of 220 V.

PV modules on the roof of the house were tilted 14° above the horizontal and the azimuth angles were −95° (East), −5° (South) and + 85° (West) in three different solar fields. The West field of 1,378 kWp, (A) with a total of 26 modules, distributed in two parallel rows of 13 modules connected in series each. The South field (B) of 3,392 kWp, with a total of 64 modules, distributed in four parallel rows of 16 modules in series each. The East field (C) of 2,703 kWp, with a total of 51 modules, distributed in three parallel rows of 17 modules also connected in serie each. Each field is connected to a Fronius inverter, model IG-30, single-phase, input voltage range between 150 V and 450 V and output voltage 230 V. The PV modules were installed on 4 cm high galvanised steel structure on slanted roof. Modules of field B have been the selected for this study, those modules have been operating for 22 years and 4 months, their useful life is 28 years and 4 months and throughout all their useful life the PV modules have been operating in Seville.

Seville is located at an altitude of 34 m above sea level and has a “Csa” climate, according to the Köppen-Geiger classification (Peel et al., 2007). Seville has a Mediterranean and subtropical climate characterized by hot, dry summer and wet and cold winters. The annual mean temperature is 19,2 °C and the monthly mean temperature ranges

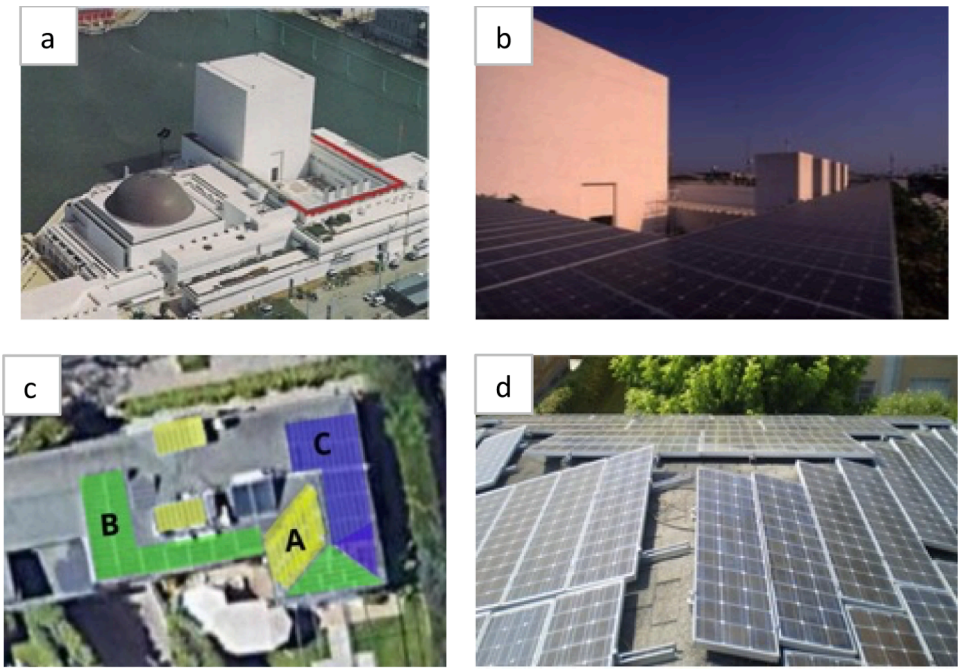

Fig. 1. General view of the two installations: Spanish Pavillion (a and b) and roof of a house (c and d) Line red in the Spanish Pavilion (10 years) (a)…Green, yelow and blue color in the roof of a house (12 years) (c). Close view of the PV modules in both installations.(b and d). (For interpretation of the references to color in this figure legend, the reader is referred to the web version of this article.)

between 10,9 °C in December and 28,2 °C in July. The annual mean relative humidity is 59%, monthly mean values range from 44% in July to 74% in December. The daily global horizontal irradiation (GHI) ranges between 3,0 kWh/m^2·day and 7,3 kWh/m^2·day (AEMET, 2020).

Visual inspection, together with EL imaging and IR thermal imaging are among the most useful methods to identify the PV modules defects (Jahn et al., 2018). Visual inspection of PV module is a useful tool also to provide us a quick view of the general condition of the PV module (cells, front and back encapsulants, frame, juntion box). Specific procedures for visual inspection based in questionnaires have been developed (Corinne et al., 2012) but the most standard method is based on the standard IEC 61215-1(2016) .In this paper, the visual inspection was performed according to the IEC 61215-1 (2016) standards and the IEA report (Köntges et al., 2017).

The infra-red thermal imaging has been performed with infrared camera Flir E6 with 160x20 pixels. The modules were grid-connected approximately at their maximum power during the measurement campaign. To complete the visual inspection and the infra-red thermal analysis, an EL imaging of the 56 PV modules was used to identify finger interruptions and affected areas due to cracked cells. For the rest realization a HAMAMATSU C11440 CCD camera and a continuous power supply for the reverse polarization of the PV modules, model XFR60-20MGA, were both used.

The I–V curves were individually measured for all the PV modules, being ensured previously that all modules were completely clean, under natural sunlight following the recommendations from the standard 60904–1 (2006). Digital multimetres were used to acquire the voltage and current signals, as well as the required meteorological variables right before and after each measurement. The module temperature is also registered, using RTD Pt100 thermal sensors with appropriate thermal coupling to the back of the modules. The global irradiance is measured with a Kipp & Zonen pyranometer, calibrated periodically to ensure the traceability of the measurements. In order to minimize measurement and conversion errors, the following conditions were imposed to all measurements: time of measurement within an hour of solar noon; global irradiance in the measurement plane higher than 820 W/m^2; the diffuse solar irradiance fraction lower than 10%; maximum variation of irradiance during time of measurement lower than 1%; wind speed lower than 0,5 m/s and a maximum variation of module temperature during time of measurement lower than 1 °C. Both sets of measurements were carried out during the month of July in 2020. The maximum relative uncertainty of the power measurements was 1%. The experimental I–V curves were translated to the standard condition using the method proposed by Bühler et al. (2014). Uncertainties for voltage and current measurements were of ± 0,01 V and ± 0,02 A respectively, 1% for the pyranometer and 0,5% for the module temperature.

Depending on the assumptions, degradation calculations may be significantly impacted. Assumptions of this study are the following:

- This study is referred to degradation rather than failure because degradation leads to lower performance but not necessary a failure.
- To assess the percentage of degradation of the module, we have no choice but to compare the measurement to the nameplate rating because we did not have the flash report of each PV module. In the 90s, PV module manufacturers usual warrant tolerances of +/-10%.
- Beginning-of-life LID effect has been considered.
- Incident irradiance has been measured using a calibrated pyranometer.
- PV modules have been cleaned, so soiling losses have not been taken into account.
- PV modules had been mounting according to Fig. 1.

3. Results and discussions

3.1. Defects

Various types of defects were detected after a thorough visual, electroluminiscence and infra-red thermal inspection of the modules. The type and frequency of the observed defects are shown in Table 1.

A more detailed explanation of these defects is the following

3.1.1. Frame defects

All the module aluminium frames were in good conditions. Nevertheless the silicone joint is cracked and the grounding screws present

Table 1
Types of defects in modules and percentage of affected modules and cells.

Type of defect (%)	% affected modules	% affected cells
Frame defects	100	NA
Junction box defects	100	NA
Defective by-pass diodes	0	NA
Hot spots	3,57	0,01
Physical impacts	5,35	0,4
Backsheet delamination and burbles	21,42	6
Darkening	100	100
Milky pattern	100	100
Cell cracks	89,29	12
Front grid and AR layer oxidation	100	100

oxidation in 100% of PV modules, as shown in Fig. 2.

3.1.2. Junction box defects

All modules have junction box conduits degraded. Another defect found is that 4% of junction boxes (2 per PV module) are bad attached to the backsheet as it is shown in Fig. 3.

During the IV measurements it was verified that none of the by-pass diodes had failed.

3.1.3. Milky pattern

EVA is the dominant encapsulant material used in the lamination of c-Si PV modules. The milky pattern is the most common type of delamination observed in all PV modules but the degree of affection is not identical among all of them. A severe milky pattern is observed on large areas over the solar cells, mainly at the proximity of the interconnection ribbons and at the cell discoloration perimeter, and, to a lesser degree, at the cell perimeter as shown in Fig. 4.

The origin of this defect could lie in a chemical reaction between the cell antireflecting coating and certain additives in the module encapsulant.

Other delamination has been observed between the cell and EVA in about 20% of the PV modules reaching about 5% of the PV cell surface. This delamination has been mainly observed at the edge of the PV cells and more frequently in the cells located at the perimeter of the PV module.

Both the selection of packaging materials and the lamination process are crucial to avoid delamination defects. But this delamination can also be affected during the exposure period by corrosion, mechanical shocks, cell breaks and entry of moisture. Compared to the packaging materials, the effect of the PV module lamination process, namely the preheating step, the curing step and the cooling step, is relatively poorly studied (Köntges et al., 2017).

3.1.4. Darkening

The darkening of EVA is a common and severe visual defect of Isofoton PV modules after 22 years under UV exposure and at elevated temperature caused by a bleaching process that could be accelerated by cracks in cells. This is a well-known problem for PV modules manufactured before the 1990 s, of EVA (Han et al., 2018). It affects 100% of the cells of 100% of the inspected modules.

Fig. 2. Frame defects: silicone joint cracked (a) and grounding screw oxidation (b).

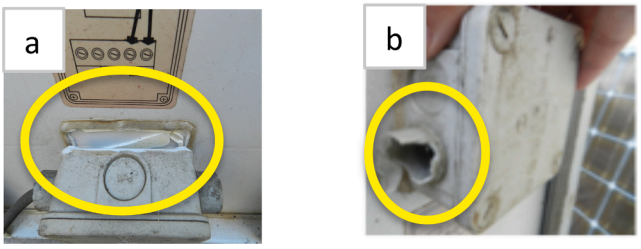

Fig. 3. Juntion box defects: Degraded conducts (a) and detached junction box (b).

This discoloration is not totally homogeneous in cells. Inside the cells, the discoloration is lower at cells perimeter. Additionally, two levels of discoloration with almost square shape have been observed. These are either a more intense discoloration inside the cells interconnection ribbons and also a squared less intense discoloration that surrounds the previous one up to approximately 0,5 cm from the cell perimeter, as shown in Figs. 5 and 6.

Moreover, cells located on the PV module perimeter tend to show a less discoloration at the cell perimeter close to the frame of the module and a greater discoloration at the cell perimeter close to the other cells. This may be due to a lower temperature of this part of the PV module in comparison to the rest due to the thermal influence of the frame, as can be seen from the thermographic analysis and is shown in Fig. 6.

IEA-PVPS TASK13-01:2014 and Jahn et al., 2018 pointed out that this is one of the most important wear-out failures of the PV modules. A likely explanation of the difference between the center and the edge of the PV module is the bleaching of EVA due to the oxygen diffusion that is more important at the edge of the module than at the center of the cells. As a result, the transmittance of EVA measured at the edge of the cell PV module is higher than at the center, for wavelengths from 380 nm to 1200 nm. However, the transmittance of EVA at the center is higher than at the edge in the wavelengths in the 300–380 nm wavelengths. This difference maybe caused because the ultravoilet absorbers in EVA in the center have been completely consumed (Pern et al., 1991). Discoloration is almost always located at the center of the cells due to a so-called "photo-bleaching" process. Photobleaching occurrs where oxygen is provided in enough quantity, been diffused through the back-sheet between cells or through cells along the cracks, to bleach the EVA that had been discolored by UV (Jordan et al., 2017a).

With the EVA discoloration the short circuit current decreases because the discoloration leads to a lower light transmissivity. Pramod Rajput et al. (2016), have found that the discoloration has a significant effect on the degradation of the module short-circuit current and hence the module power degradation but it does not affect its fill factor and open-circuit voltage. Nevertheless, when discoloration is not homogeneous over the cells, as it is the case, it impacts on the decrease of the parallel resistance and consequently on the reduction of the fill factor and open circuit voltage.

The discoloration in the cells called "snail trails", or "snail tracks", which appear as irregular dark stripes/ brownish coloured contact fingers across the cells has not be found in any module. This may be due to that this defect appears during the first years of exposure (Liu et al., 2015).

3.1.5. Cell cracks

Cell cracks have been detected during the visual inspection test when they were large enough. Micro-cracks have also been detected during the EL imaging test. A 4% percentage of the cells present visible cracks. Nevertheless 8% of the cells show micro-cracks with the EL test, distributed into 50 PV modules.

It has been observed that some cracks in the back-sheet have been located at the same location as a crack in the cell. Nevertheless, it has been observed cracks without any kind of defects at the same location in

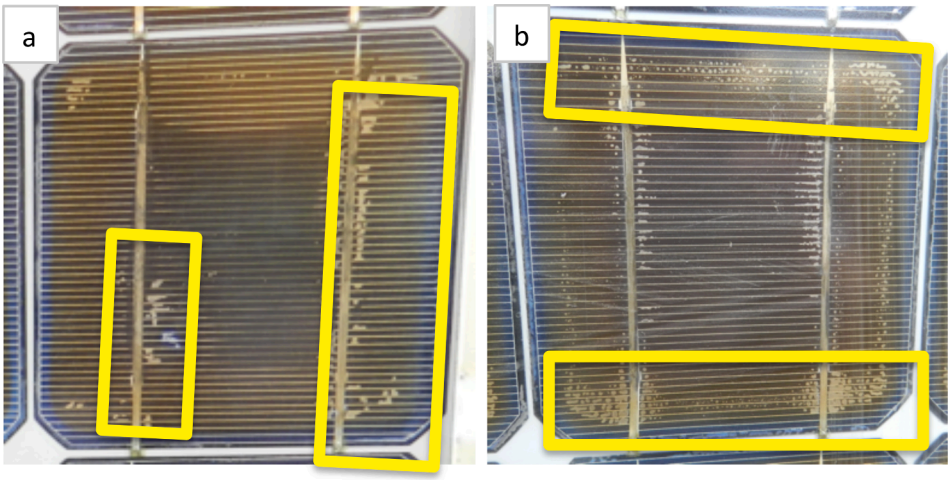

Fig. 4. Milky pattern at the proximity of the interconnection ribbons (a) and at the cell discoloration perimeter (b).

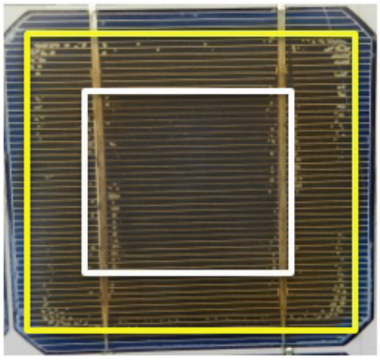

Fig. 5. Concentric discoloration levels in the cell.

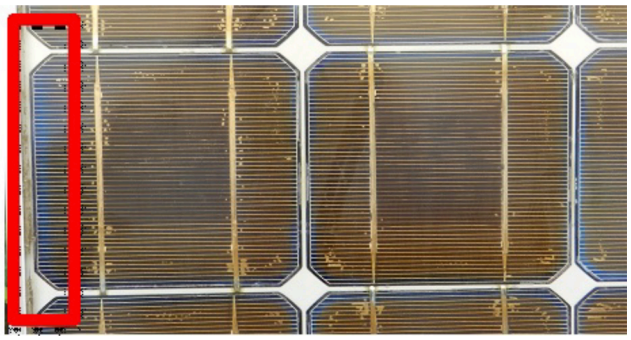

Fig. 6. Non-symetrical discoloration levels in cells located on the perimeter of the PV module (red box) and two concentric discoloration levels in both cells. (For interpretation of the references to color in this figure legend, the reader is referred to the web version of this article.)

the back-sheet. Fig. 7 shows the visual image (top) of a typical crack in the back-sheet of a module and the corresponding crack in the cell at the same location.

The cell cracks may have been formed during mechanical or thermal stresses on the cells during manufacturing, transport or bad handling during loading and unloading of the container or installation, disassemble and reassemble and the exposure period. In this study, it has been observed, Fig. 7, that about 50% of the cell cracks have just been origined in the solder point between the interconnections ribbons of two cells according to Itoh et al. (2014).

Solar cell cracks and micro-cracks are a well-known and they have a

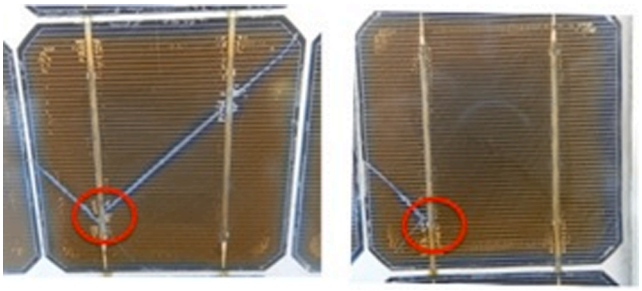

Fig. 7. Two cracked cell origined in the welding of the interconnection ribbons between two cells.

significant influence on the Pmax when the cracks leave part of the cell completely isolated (Köntges et al., 2011). In this study cracks were classified based on their size, shape, position, direction or their severity and the factors affecting them were loosely considered as two-fold: (i) those deriving from mechanical properties and (ii) those resulting from their geometrical properties.

Depending on the size, shape, position and length of the crack, the impact on the PV module performance is very different (Papargyri et al., 2020). While single cracks perpendicular to the busbars cannot electrically separate any area of the cell from the busbars, cracks parallel to the busbar may lead to high separated cell areas, up to 25% for cells with two busbars (Kajari-Schröder et al., 2011). In our research, more than 70% of the cracked cells were due to perpendicular breaks to the busbars. Fig. 8 shows the utility of the EL test to identify defects in the cells of the PV module. For instance, the cell with the yellow circle is defective. Only with a visual inspection the cell does not seem to be in bad conditions but with EL image the defect is detected. Other defects such as craked cells (red square in Fig. 8) with the non-operative part can be easily identified.

3.1.6. *Hot spots*

Two solar cells corresponding to two different PV modules, have been affected by hot spots, causing breakage of the cell and burning of the backsheet. Hot spots are caused by localized dirt, shadows, damaged cell or severe mismatch between the PV module strings. The string with the reduced short-circuit current is forced to work in inverted polarity, consuming the power generated by the other strings and potentially reaching very high temperatures (Zhang et al., 2017).

3.1.7. *Front grid and AR layer oxidation*

Front grid and AR layer oxidation have been observed in 100% of the

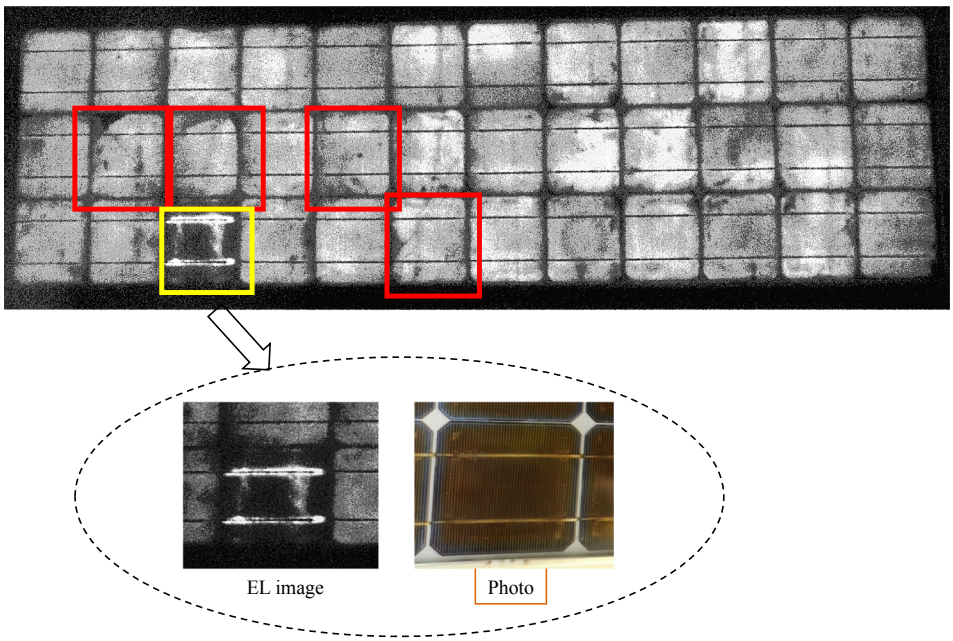

Fig. 8. Electroluminiscence image of a PV module with a PV cell photo.

cells and 100% of the analysed PV modules. This oxidation is not totally homogeneous in cells and it is reasonable to believe that the oxidation process has not stopped during the storage time of the modules (8 years).

Acetic acid is a by-product of hydrolysis within EVA that occurs in the presence of moisture, heat and UV radiation. This acetic acid acts as a catalyst in the corrosion of the cell metallization and metallic interconnects copper core and its tin coating (Gagliardi et al., 2017). The copper core causes a brown discoloration of the EVA when it is directly exposed to EVA. Usually the tin or tin-based coating and solder material should protect the copper core of the interconnect ribbon, but it may not be robust enough to resist corrosion. This metallization, or interconnection, corrosion leads to an increased series resistance and therefore losses in module performance. Due to the long diffusion paths from the encapsulant to the backsheet, acetic acid can be accumulated in front of the solar cells and lower the local pH value, leading to even faster corrosion (Kempe et al., 2007; Köntges et al., 2017).

The oxidation process has been accentuated over the last 10 years, cells show two concentric squares, the inside one shows greater decay and corrosion than the perimeter square. This impact is observed in all cells of all PV modules.

3.1.8. Physical impacts

Physical impacts could result in breakage of the glass or cracks of the backsheet. These physical impacts are generally caused by weather, mishandling upon relocation or major thermal expansion mismatches. Three modules with physical impacts in the backsheet but neither in the glass nor junction box have been observed. In two of those modules, the cell on the front side is cracked too.

3.1.9. Backsheet delamination, bubbles.

In 14,29% of the PV modules bubbles were observed and in 7,14% of the PVmodules delamination of the backsheet was detected as shown in Fig. 9. This delamination took place at the interface between the outer PVF and the PET, and between the PET and the inner PVF, mainly in the place of the junction box, but not only there. The inner PVF remained well attached to the EVA. This could indicate a stability problem of the proprietary adhesive used at the backsheet. In general, delamination defects depend on encapsulant materials, climate and exposure time (Julien et al., 2020)

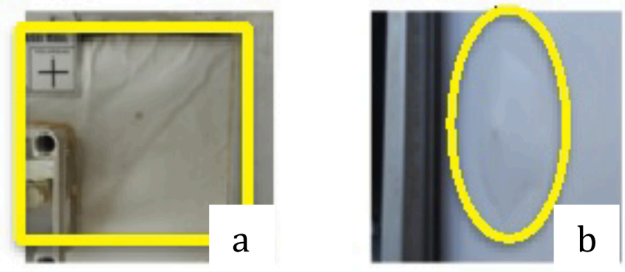

Fig. 9. Backsheet delamination (a) and bubble (b).

3.2. Electrical performance

The original actual power output of the PV modules is assumed to be ± 10% of the nameplate value as it was typical at the time of manufacturing of these modules. Without any more reliable data about the initial power output, we accept the uncertainty on the power loss that is calculated as the difference between the measured output and the nameplate value.

Fig. 10 shows in a column the degradation percentages of Pmax, and in another column the degration percentages of Isc, Voc and FF for all the 56 PV modules analyzed.

Fig. 10 shows that the degradation of the maximum power of most of the analysed PV modules is due to a greater extent to the short-circuit current degradation, followed by the degradation of the fill factor and the open circuit voltage. Likewise, it has been obtained that the Pmax value shows an average degradation of 30,9% throughout the 22 operation years, having a maximum of 38,0% and a minimum of 22,2%, which corresponds at an annual ratio between 1,0–1,7%/year with an average of 1,4%/year. Moreover, the average degradation of the Isc has been 16,4%, which corresponds to an annual ratio between 0,4–1,0%/year with an average annual ratio of 0,8%/year. The average FF degradation has been 13,0%/year which corresponds to an annual ratio between 0,3–0,9%/year, with an average annual ratio of 0,6%/year. The Voc average degradation has been 4,9%, which corresponds to an annual ratio between 0,1–0,5%/year, with an average annual ratio of 0,2%/year.

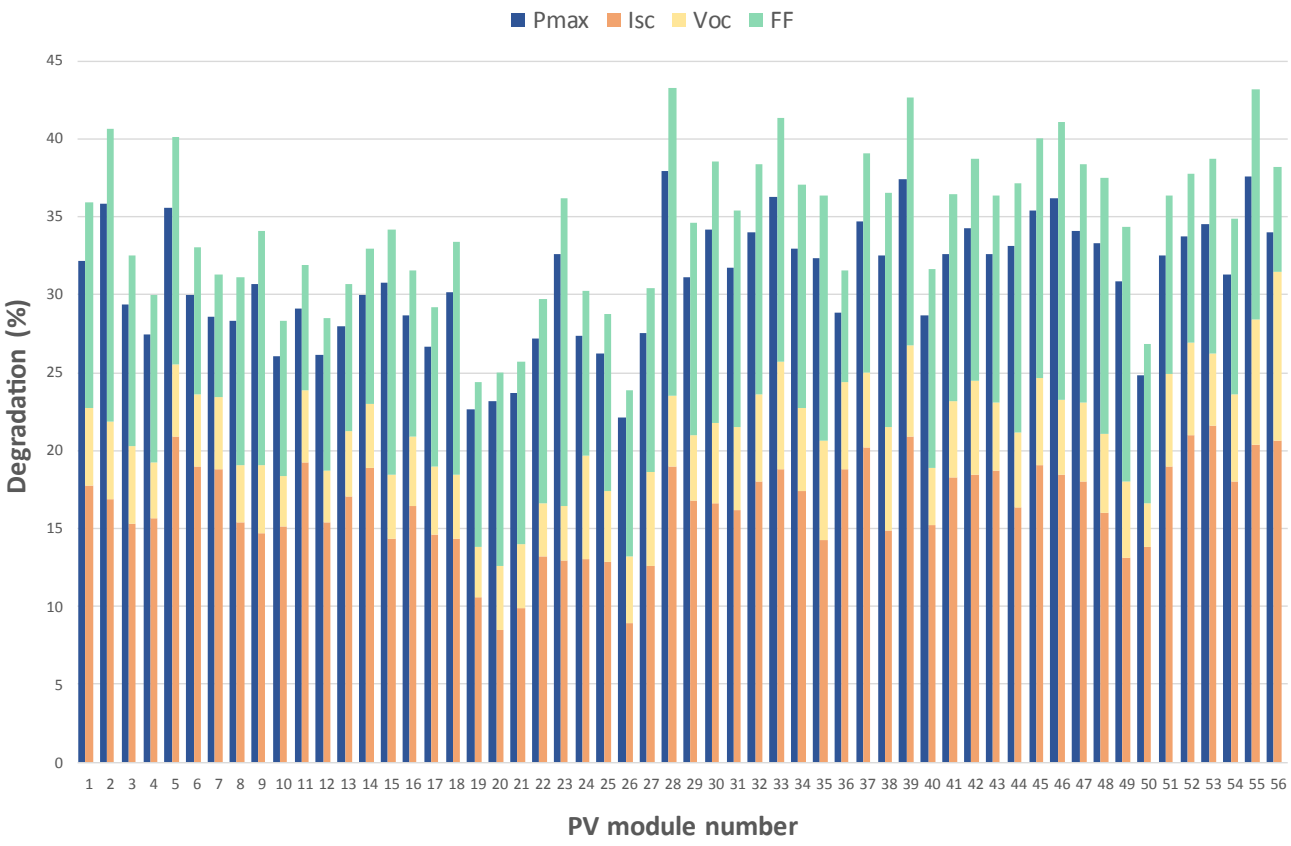

Fig. 10. Total degradation percentage of the 56 PV modules (2 bars for each module). In the dark blue bar Pmax, in the other bar in orange, yellow and green colors, Isc, Voc and FF degradation respectively. (For interpretation of the references to color in this figure legend, the reader is referred to the web version of this article.)

The loss of short-circuit current could be partially related to the loss of optical coupling at the cell-encapsulant interface originated by the milky pattern delamination, the front delamination, the degradation of the AR coating layer, cracked cells and an inherent degradation of the p–n junction, related to the cell process fabrication, which has been described by several studies carried out at IEA, task 13:2014 (Köntges et al., 2014).

The loss of open circuit voltage could be related to corrosion between cell interconnections, short circuits of one cell with another or even a failure in the by-pass diode. It could also be due to the effect of light induced degradation (LID) or potential induced degradation (PID). For example, module No. 50 (676) has less corrosion compared to others, milky pattern and a broken cell, but without cell short circuits.

Fig. 11 shows the electrical parameters dispersion of the PV modules, (a) maximum power, (b) short circuit current, (c) open circuit voltage and (d) fill factor.

4. Comparative analysis

There are three PV modules degradation studies from the same manufacturer, with the same cell and the same encapsulant, located in three different locations with very similar climates and with different number of operation years, 12 years (Sanchez-Friera et al., 2011), 15 years (Ferreira da Fonseca et al., 2020) and 17 years (Moreton et al., 2013).

Table 2 shows the operating and testing conditions and defects found in the four studies. All of them are based in m-C-Si PV cells, size 103x103 mm and of the same manufacturer, Isofotón.

The works selected for comparison with this study analyse different locations but these fall within the same climatic classification as Seville, type Csa, according to Köppen-Geiger (Peel et al., 2007) except Porto Alegre which has Cfa climatic classification. According to IEA-PVPS T13-09 (2017) (Köntges et al., 2017) the climatic conditions covered with Köppen-Geiger groups are covering temperature and humidity stress which does not cover all important stress factors for the application in PV degradation studies such as UV irradiance, soiling, temperature cycling, humidity. The temporal resolution of the data are annual and monthly averages that seems too low. In this case, Malaga and Porto Alegre are in the coastal zone. Madrid has a colder and drier climate than Malaga and Seville. Relative humidity in Malaga is slightly higher than Madrid and Seville.

It is noteworthy that in the Porto Alegre and Madrid studies a calibrated cell and a module have been used to measure global irradiance instead of a pyranometer, which can lead to an underestimation of irradiance (Lillo-Bravo et al., 2020). In addition, not all the studies have the same reference, there are studies that degradation rates are referenced to nameplate, other to initial measurements rating as reference, other use indoor with solar simulators or outdoor measurement conditions (Jordan et al., 2016).

The main difference found is that as the number of years of operation increase, around 20 years, the presence of severe and higher percentage of oxidation of the metallization, discoloration of EVA and milky pattern stands out. In the other studies, these effects are not severe or are not even detected, as is the case of oxidation and delamination in Madrid.

The factors that difficult the evaluation of the degradation rate are due to the uncertainties associated to the measurement of the electric and climatic parameters, the extrapolation uncertainty of the Pmax from experimental conditions to standard conditions and the initial measurement reference (if is a nameplate, with or wihout LID effects, …). Typically, a good measurement of electric parameters has uncertainty values lower than 1%-2%. The irradiance is the major source of uncertainty and affects directly the short-circuit current. However, maximum

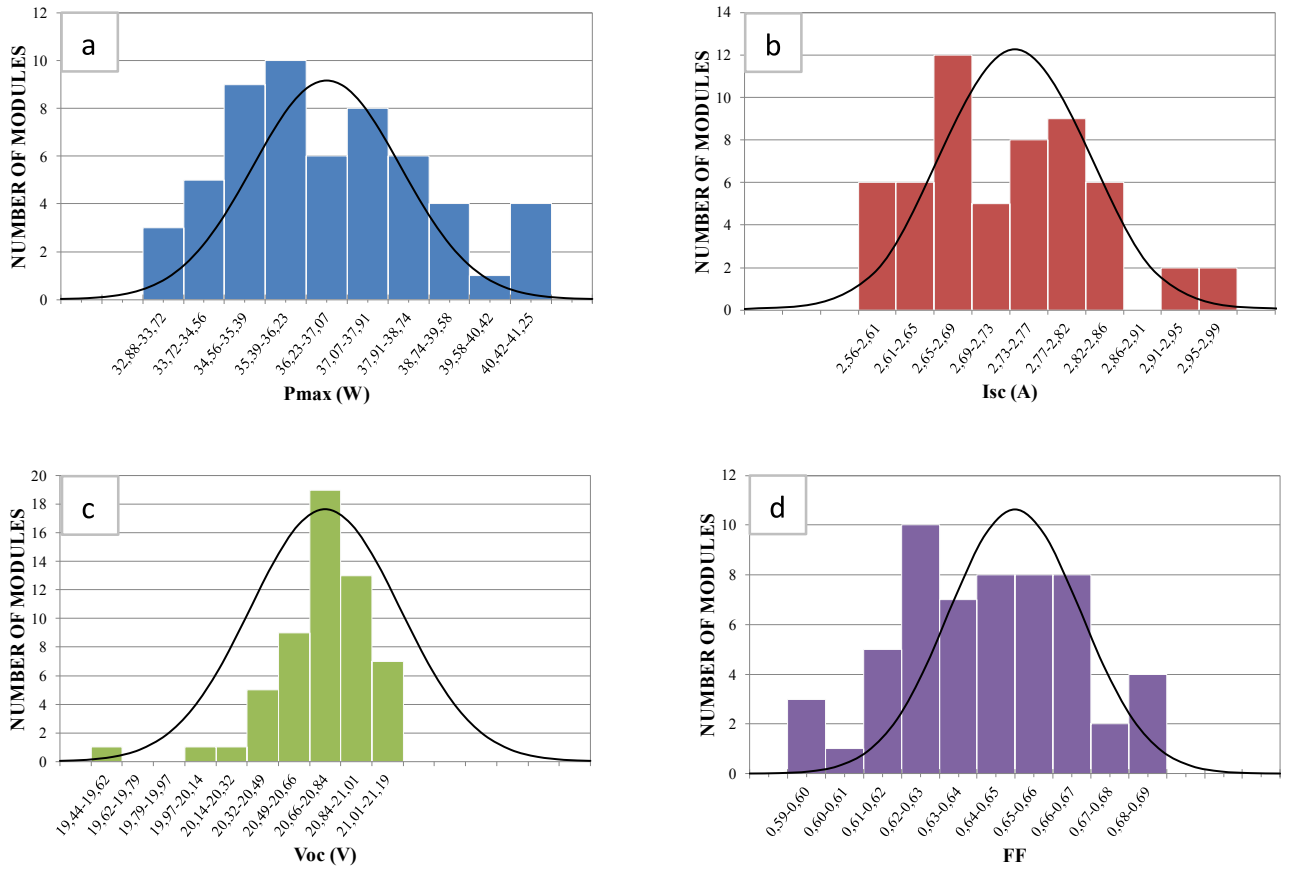

Fig. 11. Degradation rates dispersion parameters after 22 years of outdoor exposition. (a) Maximum power, (b) Short circuit current, (c) Open circuit voltage and (d) Fill factor.

power is the most sensitive parameter, because it suffers simultaneous interference from climatic paramters (irradiance and temperature) and electric parameters in the initial and final measurement periods.

Table 3 shows the total degradation and the annual mean ratio of Pmax, Voc, FF and Isc in the current study and in the other three research works.

For the four studies, it is observed that there is difference among the annual average maximum power degradation rates with the operation years. In all the studies the decrease in the short-circuit intensity is the parameter that has suffered the most reduction, fundamentally based on the defects of the encapsulant browning and the antireflective layer degradation. The low rate degradation of Pmax in Madrid with respect to the other studies can be explained by the absence of oxidation and delamination, while in Malaga and Porto Alegre reports this has not been highlighted.

However, although all studies show discoloration symptoms, as the operating time increases, the severity of discoloration, cell oxidation and milky pattern increases. Fig. 12 shows the appearance of the cell in three of the four studies. With these images, the difference in the severity of discoloration, milky pattern, and especially of oxidation of cell and interconnects. According to the IEA-PVPS T13-09: 2017 (Köntges et al., 2017) and Ferreira da Fonseca et al. (2020), oxidation defects exponentially affect degradation and would partly explain the higher degradation rate in our study, added to the FF and Voc degration rate.

These differences in defects together with others such as cell crack show that when the defects tend to be more severe, the degradation grows in a non-linear way. This coherent with what is indicated in the IEA-PVPS T13-09: 2017 (Köntges et al., 2017).

This is confirmed in other degradation studies that contemplate more than 20 years of operation, such as in Pramod et al. (2016) where the Pmax degradation rate has been found with average value 1,9%/year, or in Chandel et al. (2015) where the Pmax degradation rate has been found with average value 1,4%/year. In those cases, and in our study a severe discoloration and the corrosion in busbar, string interconnection ribbon, cell interconnection ribbon is a commonly observed as defects in all PV modules that have been increasing with the time. That is reflected in a more significant degradation, not only in Isc, but in the FF and Voc, and consequently in the Pmax. This is in accordance with IEA-PVPS T13-09: 2017 (Köntges et al., 2017), confirming that severe degradation is frequently observed in PV modules subjected to outdoor exposure conditions over 20 years. So, degradation rates based on the assumption of linearity may not be sufficiently accurate (Jordan et al., 2017a). In the initial period of operation, about the first year, degradation rates tend to be higher than in the middle-period of the operating life due to the stronger action of specific degradation modes, such as LID (Ishii and Masuda, 2017). During the wear-out period of operation, approximately more than 20 years, degradation rates tend to be higher due to the stronger action of corrosion and to the severity of the defects.

5. Conclusions

The analysis of the degradation mechanisms of 56 PV modules after 22 years of exposure and its comparison with other three research works has been presented. PV modules inspection revealed severe damage of junction box tubes, golden brownish discoloration, delamination of encapsulant with severe milky pattern, oxidation of front grid metal fingers, busbar and AR layer. To a lesser extent, delamination and bubbling in back sheet. Degradation of power output of PV modules reached a total value of 30,89% and a mean annual value of 1,4%. This is attributed to a loss in short circuit current, but also to losses in open circuit voltage and fill factor.

There is a significant difference between most studies of degradation

Table 2
Comparison of operating and testing conditions and defects.

Reference	Present study	Moreton et al. (2013)	Ferreira da Fonseca et al. (2020)	Sanchez-Friera et al. (2011)
Location (Longitude, Latitude, altitude)	Seville, (Spain). (37,4N, 5,9W, 16 m)	Madrid, (Spain). (40,5N, 3,7W, 667 m)	Porto Alegre (Brasil). (30,0S, 51,2W, 1 m)	Malaga, (Spain). (36,7N, 4,4W, 4 m)
Operation period	22 years	17 years	15 years	12 years
Köppen- Geiger Classification	Csa	Csa	Cfa (Humid temperate climate with hot summer)	Csa
Sample	56 PV modules 53 Wp, 36 cells.	76 PV modules 90 Wp, 60 cells,	48 PV modules 100 Wp, 72 cells.	42 PV modules 53 Wp, 36 cells.
Testing	Visual, Thermography, EL and I-V curve.	Visual, Thermography, Electrical insolation and I-V curve.	Visual, thermography, Electrical insolation, EL and I-V curve. EL, thermography and Electrical insulation were applied only a sample of eight modules.	Visual, Thermography and I-V curve.
Mesaurement	Outdoor, Kipp & Zonen pyranometer. Uncertainties for voltage and current measurements were of ± 0.01 V and ± 0.02 A, respectively The curves were translated to standard test conditions (STC) following the procedure described by Bühler et al. (2014).	Indoor, reference PV modules. Uncertainty of the power measurements is not shown. The curves were translated to standard test conditions (STC) following the Procedure 1 described in IEC 60891 (2009).	Outdoor, reference cell. Uncertainties for voltage and current measurements were of ± 0.01 V and ± 0.02 A, respectively The curves were translated to standard test conditions (STC) following the procedure described by Bühler et al. (2014).	Outdoor, Kipp & Zonen pyranometer. Uncertainty of the power measurements was 2% at the beginning of the period under study and 1% at the end. The curves were translated to standard test conditions (STC) following the Procedure 1 described in IEC 60891 (2009).
Defects:	Darkening: 100% Milky pattern: 100% Oxidation: 100% Module with cell cracks: 89,29% Backsheet delamination 21,42% Junction box: 100%	Cracks in the junction boxes :7% Backsheet delamination: 69% Darkening.: 83% Cracks frame joint :37%.	Milky pattern 79,2% Darkening: 100% Oxidation 100% Cell cracks 27%. Backsheet delamination: 2,1%.	Milky pattern: 93% Oxidation :100% Cell cracks: 60% Backsheet delamination 7% Junction box: 100%
Relevant defects:	Severe oxidation of the metallization and discoloration of EVA. Severe milky pattern. Many cell cracks.	Backsheet delamination at the polyester/ polyvinyl fluoride outer interface and cracks in the terminal boxes and at the joint between the frame and the laminate	Oxidation of the metallization and discoloration of EVA. Milky pattern.	Loss of adhesion strength at the cell-encapsulant interface and the degradation of the AR coating layer.
Author comments:	Severe defects.	They have not observed front delamination (milky pattern) or grid oxidation.	Encapsulant darkening and the anti-reflective layer degradation, contribute significantly to the reduction of short circuit current.	Oxidation of the metallization grid does not seem to have any impact on the performance. Glass soiling has minor impact.

Table 3
Main parameters of the total degradation rates and annual average degradation rates of the PV modules for the 4 studies.

Reference	Present study		Sánchez Friera et al. (2011)		Moretón et al. (2013)		Ferreira da Fonseca et al. (2020)	
Location	Seville, (Spain).		Madrid, (Spain).		Porto Alegre (Brasil).		Malaga, (Spain).	
Operation period	22 years		17 years		15 years		12 years	
	Total Degradation (%)	Average annual rate (%)	Total Degradation (%)	Average anual rate (%)	Total Degradation (%)	Average anual rate (%)	Total Degradation (%)	Average Annual rate (%)
Pmax/Rate	−30,9	−1,4	−11,5	−0,96	−9/	−0,53	−9,5	−0,63
Voc/ Rate	−4,9	−0,2	−1,9	−0,16	−1,2/	−0,07	−0,1	−0,01
FF/Rate	−13,0	−0,6	−0,7	−0,06	+0,1/	0,01	+0,77	+0,05
Isc/Rate	−16,4	−0,8	−9,3	−0,78	− 8/	−0,47	−9,12	−0,61

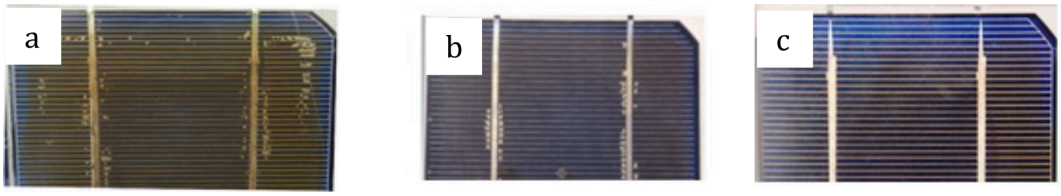

Fig. 12. Visual appearance of a cell after 22 years of operation (this study, photo a), compared with a similar cell after 15 years (Ferreira da Fonseca et al., 2020, photo b) and 12 years of operation (Sanchez-Friera et al., 2011, photo c).

rates applied to shorter and higher exposure time periods of around 20 years, nearly to warranty period limit. The severity of the discoloration, milky pattern and oxidation processes significantly increases the average degradation rates in studies applied over 20 years. Electroluminiscence test has identified in even greater detail cracked cells and the effect on the inactive zone of the cell.

It is important to highlight that the tested modules were manufactured in the 90 s and are made up by thick and small cells (about 300 μm and 103x103 mm^2, surface) compared with current PV modules in which cells are three times thinner (about 100 μm) and their sizes are larger (up to 200 × 200 mm). Cells analysed in the current review are embedded in small PV modules of approximate surface of 0,5 m^2, while current cells are assembled in PV modules up to 4 times larger. This suggests that although manufacturing processes have improved and have been automated with respect to those used in the 1990 s, the mechanical or thermal stresses on the cells during shipping, transportation (Hsu et al., 2016), assembly process and the exposure period can make a large number of microcracks that should be prevented, making electroluminescence inspection in each step of the installation process and also the adaptation of standards to this new situation.

Declaration of Competing Interest

The authors declare that they have no known competing financial interests or personal relationships that could have appeared to influence the work reported in this paper.

References

AEMET. Valores climatologicos. 2020. Agencia estatal de meteorologia. http://www.aemet.es/es/serviciosclimaticos/datosclimatologicos/valoresclimatologicos?l=5783&k=. Access on line on 26th July 2020.

Berardone, I., Lopez Garcia, J., Paggi, M., 2018. Analysis of electroluminescence and infrared thermal images of monocrystalline silicon photovoltaic modules after 20 years of outdoor use in a solar vehicle. Sol. Energy. 173, 478–486.

Braisaz, B., Duchayne, C., VanIseghem, M., Radouane, K., 2014. PVaging model applied to several meteorological conditions. Proc. 29th PVSEC Proc., Amsterdam, The Netherlands. 2303–2309.

Bühler, A.J., Perin Gasparin, F., Krenzinger, A., 2014. Post-processing data of measured I-V curves of photovoltaic devices. Renew. Energy 68, 602–610.

Chandel, S.S., Naik, M.N., Sharma, V., Chandel, R., 2015. Degradation analysis of 28 years field exposed mono-c-Si photovoltaic modules of a direct coupled solar water pumping system in western Himalayan region of India. Renew. Energy. 78, 193–202.

Corinne, E., et al., 2012. Development of a Visual Inspection Data Collection Tool for Evaluation of Fielded PV Module Condition. National Rewenable Energy Laboratory (NREL).

Dubey, R., Chattopadhyay, S., Kuthanazhi, V., John, J., Solanki, C., Kottantharayil, A., Arora, B., Narasimhan, K., Kuber, V., Vasi, J., 2013. All-India India Survey of Photovoltaic Module Degradation: 2013. Mumbai, India.

Ferreira da Fonseca, J.E., Schuck de Oliveira, F., Massen Prieb, C.W., Krenzinger, A., 2020. Degradation analysis of a photovoltaic generator after operating for 15 years in southern Brazil. Sol. Energy 196, 196–206.

Gagliardi, M., Lenarda, P., Paggi, M., 2017. A reaction-diffusion formulation to simulate EVA polymer degradation in environmental and accelerated ageing conditions. Sol. Energy Mater. Sol. Cells. 164, 93–106.

Gu, X., Lyu, Y., Yu, L.-C., Lin, C.-C., Stanley, D., 2015. Effect of inten- sity and wavelength of spectral UV light on discoloration of laminated Glass/EVA/PPE PV module. 3rd Atlas-NIST Workshop PV Mater. Durability.

Han, H., Dong, X., Li, B., Yan, H., Verlinden, P.J., Liu, J., Huang, J., Liang, Z., Shen, H., 2018. Degradation analysis of crystalline silicon photovoltaic modules exposed over 30 years in hot-humid climate in China. Sol. Energy 170, 510–519.

IEC 60891:2009. International Electrotechnical Commission. Photovoltaic devices - Procedures for temperature and irradiance corrections to measured I-V characteristics.

IEC 61215-1:2016. International Electrotechnical Commission.Terrestrial photovoltaic (PV) modules - Design qualification and type approval - Part 1: Test requirements.

IEC 61215-1-1:2016. International Electrotechnical Commission. Terrestrial photovoltaic (PV) modules. Design qualification and type approval. Part 1-1: Special requirements for testing of crystalline silicon photovoltaic (PV) modules.

IEC 61215-1-2: 2016. International Electrotechnical Commission.Terrestrial photovoltaic (PV) modules - Design qualification and type approval - Part 1-2: Special requirements for testing of thin-film Cadmium Telluride (CdTe) based photovoltaic (PV) modules.

IEC 61215-1-3: 2016. International Electrotechnical Commission.Terrestrial photovoltaic (PV) modules - Design qualification and type approval - Part 1-3: Special requirements for testing of thin-film amorphous silicon based photovoltaic (PV) modules.

IEC 61215-1-4: 2016. International Electrotechnical Commission.Terrestrial photovoltaic (PV) modules - Design qualification and type approval - Part 1-4: Special requirements for testing of thin-film Cu (In GA) (S, Se) 2 based photovoltaic (PV) modules.

IEC 61215-2:2016. International Electrotechnical Commission. Terrestrial photovoltaic (PV) modules - Design qualification and type approval - Part 2: Test procedures.

International Energy Agency, 2019. Renewables. IEA, Paris https://www.iea.org/reports/renewables-2019.

Ishii, T., Masuda, A., 2017. Annual degradation rates of recent crystalline silicon photovoltaic modules. Prog. Photovolt. Res. Appl. 25 (12), 953–967.

Itoh, U., Yoshida, M., Tokuhisa, H., Takeuchi, K., Takemura, Y., 2014. Solder Joint Failure Modes in the Conventional Crystalline Si Module. Energy Procedia 55, 464–468.

Jahn, U., Herz, M., Köntges, M., Parlevliet, D., Paggi, M., Tsanakas, I., Stein, J.S., Berger, K.A., Ranta, S., Roger, H., Richter, M., Tanahashi, T., 2018. Review on Infrared and Electroluminescence Imaging for PV Field Applications. International Energy Agency. IEA PVPS Task 13, Subtask 3.3 Report IEA-PVPS T13-10:2018. ISBN 978-3-906042-53-4.

Jordan, D.C., Kurtz, S.R., VanSant, K., Newmiller, J., 2016. Compendium of photovoltaic degradation rates. Prog. Photovolt. Res. Appl. 24 (7), 978–989.

Jordan, D.C., Silverman, T.J., Sekulic, B., Kurtz, S.R., 2017a. PV degradation curves: non linearities and failure modes. Prog. Photovolt: Res. Appl. 25 (7), 583–591.

Jordan, D.C., Silverman, T.J., Wohlgemuth, J.H., Kurtz, S.R., VanSant, K.T., 2017b. Photovoltaic failure and degradation modes. Prog. Photovolt. Res. Appl. 25 (4), 318–326.

Jorgensen, G., Terwilliger, K., Glick, S., Pern, J., McMahon, T., 2003. Materials Testing for PV Module Encapsulation. NREL/CP-520-33578. Contract No. DE-AC36-99-GO10337.

Julien, S.E., Kempe, M.D., Eafanti, J.J., Morse, J., Wang, Y.u., Fairbrother, A., Napoli, S., Hauser, A.W., Ji, L., O'Brien, G.S., Gu, X., French, R.H., Bruckman, L.S., Wan, K.-T., Boyce, K.P., 2020. Characterizing photovoltaic backsheet adhesion degradation using the wedge and single cantilever beam tests, Part I: Field Modules. Sol. Energy Mater. Sol. Cells 215, 110669. https://doi.org/10.1016/j.solmat.2020.110669.

Kajari-Schröder, S., Kunze, I., Eitner, U., Köntges, M., 2011. Spatial and orientational distribution of cracks in crystalline photovoltaic modules generated by mechanical load tests. Sol. Energy Mater. Sol. Cells 95 (11), 3054–3059.

Kempe, M.D., Jorgensen, G.J., Terwilliger, K.M., McMahon, T.J., Kennedy, C.E., Borek, T. T., 2007. Acetic acid production and glass transition concerns with ethylene-vinylacetate used in photovoltaic devices. Sol. Energy Mater. Sol. Cells. 91 (4), 315–329.

Köntges, M., Kunze, I., Kajari-Schröder, S., Breitenmoser, X., Bjørneklett, B., 2011. The risk of power loss in crystalline silicon based photovoltaic modules due to micro-cracks. Sol. Energy Mater. Sol. Cells 95 (4), 1131–1137.

Köntges, M., Kurtz, S., Packard, C., Jahn, U., Berger, K.A., Kato, K., Friesen, T., Liu, H., Van Iseghem, M., 2014. Review of Failures of Photovoltaic Modules. International Energy Agency. IEA PVPS Task 13. External final report IEA-PVPS March 2014. ISBN 978-3-906042-16-9.

Köntges, M., Oreski, G., Jahn, U., Herz, M., Hacke, P., Weiss, K., Razongles, G., Parlevliet, D., Paggi, M., Tanahashi, T., French, R.H., 2017. Assessment of Photovoltaic Module Failures in the Field. International Energy Agency. IEA PVPS Task 13. Subtask 3 Report IEA-PVPS T13–09:2017 May 2017 ISBN 978-3-906042-54-1.

LG.2020.https://www.lg.com/us/business/download/resources/BT00002151/BT00002151_2573.pdf. Access on line on 24th August 2020.

Lillo-Bravo, I., González-Martínez, P., Larrañeta, M., Guasumba-Codena, J., 2018. Impact of Energy Losses Due to Failures on Photovoltaic Plant Energy Balance. Energies. 11 (2), 363. https://doi.org/10.3390/en11020363.

Lillo-Bravo, I., Larrañeta, M., Núñez-Ortega, E., González-Galván, R., 2020. Simplified model to correct thermopile pyranometer solar radiation measurements for photovoltaic module yield estimation. Renewable Energy 146, 1486–1497.

Lindig, S., Kaaya, I., Weiss, K.-A., Moser, D., Topic, M., 2018. Review of Statistical and Analytical Degradation Models for Photovoltaic Modules and Systems as Well as Related Improvements. IEEE J. Photovoltaics 8 (6), 1773–1786.

Moreton, R., Pigueiras, E., Zilles, R., Gomez, T., Martinez de Olcoz, A., 2013. Performance analysis of a 7-kW crystalline silicon generator after 17 years of operation in Madrid. Prog. Photovoltaics Res. Appl. 22.

Mussard, M., Amara, M., 2018. Performance of solar photovoltaic modules under arid climatic conditions: A review. Sol. Energy 174, 409–421.

Ndiaye, A., Charki, A., Kobi, A., Kébé, C.M.F., Ndiaye, P.A., Sambou, V., 2013. Degradations of silicon photovoltaic modules: A literature review. Sol. Energy 96, 140–151.

Pan, R., Kuitche, J., Tamizhmani, G., 2011. Degradation analysis of solar photovoltaic modules: Influence of environmental factor. Proc. Annu. Rel. Maintainability Symp. 1–5.

Papargyri, L., Theristis, M., Kubicek, B., Krametz, T., Mayr, C., Papanastasiou, P., Georghiou, G.E., 2020. Modelling and experimental investigations of microcracks in crystalline silicon photovoltaics: A review. Renewable Energy 145, 2387–2408.

Peel, M.C., Finlayson, B.L., McMahon, T.A., 2007. Updated world map of the Köppen-Geiger climate classification. Hydrol. Earth Syst. Sci. 11 (5), 1633–1644.

Pern, F. J., Czanderna, A. W., Emery, K., A., Dhere, R. G., 1991. Weathering degradation of EVA encapsulant and the effect of its yellowing on solar cell efficiency. The Conference Record of the Twenty-Second IEEE Photovoltaic Specialists Conference, Las Vegas, NV, USA. 1, 557-561.

Rajput, Pramod, Tiwari, G.N., Sastry, O.S., Bora, Birinchi, Sharma, Vikrant, 2016. Degradation of mono-crystalline photovoltaic modules after 22 years of outdoor exposure in the composite climate of India. Sol. Energy 135, 786–795.

Sánchez-Friera, Paula, Piliougine, Michel, Peláez, Javier, Carretero, Jesús, Sidrach de Cardona, Mariano, 2011. Analysis of degradation mechanisms of crystalline silicon PV modules after 12 years of operation in Southern Europe. Prog. Photovolt: Res. Appl. 19 (6), 658–666.

Sharma, Vikrant, Sastry, O.S., Kumar, Arun, Bora, Birinchi, Chandel, S.S., 2014. Degradation analysis of a-Si, (HIT) hetro-junction intrinsic thin layer silicon and m-C-Si solar photovoltaic technologies under outdoor conditions. Energy. 72, 536–546.

Liu, Han-Chang, Huang, Chung-Teng, Lee, Wen-Kuei, Yan, Shih-Siang, Lin, Fu-Ming, 2015. A Defect Formation as Snail Trails in Photovoltaic Modules. Energy and Power Engineering. 07, 348–353.

Hsu, Shu-Tsung, Long, Yean-San, Wu, Teng-Chun, 2016. A new test method for shipping pallets of solar products. Transactions of the Canadian Society for Mechanical Engineering. 40 (4), 481–489.

SUNPOWER. 2020. https://us.sunpower.com/sites/default/files/media-library/warranties/wr-sunpower-residential-dc-module-warranty-na-503170.pdf. Access on line on 24th August 2020.

Zhang, Z., Shan, L., Wang, L., Wu, J., Quan, P., Jiang, M., 2017. Study on case analysis and effect factors of hot spot failure for photovoltaic module. Taiyangneng Xuebao/Acta Energiae Solaris Sinica. 38, 271–278.

Zimmermann, Claus G., 2008. Time dependent degradation of photovoltaic modules by ultraviolet light. Applied Physics Letter. 92 (24), 241110. https://doi.org/10.1063/1.2947589.